

# Domain Walls Zoo in Supersymmetric $QCD$

A.V. Smilga<sup>1, 2</sup> and A.I. Veselov<sup>1</sup>

## Abstract

Solving numerically the equations of motion for the effective lagrangian describing supersymmetric  $QCD$  with the  $SU(2)$  gauge group, we find a menagerie of complex domain wall solutions connecting different chirally asymmetric vacua. Some of these solutions are BPS-saturated walls; they exist when the mass of the matter fields does not exceed some critical value  $m < m_* = 4.67059\dots$ . There are also sphaleron branches (saddle points of the energy functional). In the range  $m_* < m < m_{**} \approx 4.83$ , one of these branches becomes a local minimum (which is *not* a BPS - saturated one). At  $m > m_{**}$ , the complex walls disappear altogether and only the walls connecting a chirally asymmetric vacuum with the chirally symmetric one survive.

---

<sup>1</sup>ITEP, B. Chermushkinskaya 25, Moscow 117218, Russia

<sup>2</sup>Service de Physique Théorique de Saclay, 91191 Gif-Sur-Yvette, France

# 1 Introduction

Supersymmetric QCD is the theory involving (in a simplest version) a gauge vector supermultiplet  $V$  and a couple of chiral matter supermultiplets  $Q^f$  belonging to the fundamental representation of the gauge group  $SU(N)$ . The lagrangian of the model reads

$$\mathcal{L} = \left( \frac{1}{4g^2} \text{Tr} \int d^2\theta W^2 + \text{H.c.} \right) + \frac{1}{4} \int d^2\theta d^2\bar{\theta} \bar{S}^f e^V S^f - \left( \frac{m}{4} \int d^2\theta S^f S_f + \text{H.c.} \right), \quad (1.1)$$

where  $S_f = \epsilon_{fg} S^g$  (for further conveniences, we have changed a sign of mass here compared to the standard convention). The dynamics of this model is in many respects similar to the dynamics of the standard (non-supersymmetric) QCD and, on the other hand, supersymmetry allows here to obtain a lot of exact results [1].

Like in the standard QCD, the axial  $U_A(1)$  symmetry corresponding to the chiral rotation of the gluino field and present in the tree-level lagrangian (1.1) is broken by anomaly down to  $Z_{2N}$ . This discrete chiral symmetry can be further broken spontaneously down to  $Z_2$  so that the chiral condensate  $\langle \text{Tr} \{ \lambda^\alpha \lambda_\alpha \} \rangle$  ( $\lambda_\alpha$  is a two - component Weyl spinor describing the gluino field) is formed. There are  $N$  different vacua with different phases of the condensate

$$\langle \text{Tr} \lambda^2 \rangle = \Sigma e^{2\pi i k/N}, \quad k = 0, \dots, N-1 \quad (1.2)$$

It was noted recently [2] that on top of  $N$  chirally asymmetric vacua (1.2), also a chirally symmetric vacuum with zero value of the condensate exists.

The presence of different degenerate physical vacua in the theory implies the existence of domain walls — static field configurations depending only on one spatial coordinate ( $z$ ) which interpolate between one of the vacua at  $z = -\infty$  and another one at  $z = \infty$  and minimizing the energy functional. As was shown in [3], in many cases the energy density of these walls can be found exactly due to the fact that the walls present the BPS-saturated states. The key ingredient here is the central extension of the  $N = 1$  superalgebra [3, 4]

$$\{ \bar{Q}_{\dot{\alpha}} \bar{Q}_{\dot{\beta}} \} = 4 (\vec{\sigma})_{\dot{\alpha}\dot{\beta}} \int d^3x \vec{\nabla} \left\{ \left[ -\frac{m}{2} S^f S_f + \frac{1}{16\pi^2} \text{Tr} W^2 \right] - \frac{N}{16\pi^2} \text{Tr} W^2 \right\}_{\theta=0}, \quad (1.3)$$

A domain wall is a configuration where the integral of the full derivative in the RHS of Eq.(1.3) is non-zero so that the standard  $N = 1$  SUSY algebra in the wall sector is modified. A BPS-saturated wall is a configuration preserving 1/2 of the original supersymmetry i.e. a configuration annihilated by the action of two certain real linear combinations of the original complex supercharges  $Q_\alpha, \bar{Q}^{\dot{\alpha}}$ <sup>3</sup>.

<sup>3</sup>Such BPS-saturated walls were known earlier in 2-dimensional supersymmetric theories (they are just solitons there) [5, 6] and were considered also in 4-dimensional theories in stringy context [7].

Combining (1.3) with the standard SUSY commutator  $\{Q_\alpha, \bar{Q}^\beta\} = 2(\sigma_\mu)_\alpha^\beta P_\mu$  and bearing in mind that the vacuum expectation value of the expression in the square brackets in Eq.(1.3) is zero due to Konishi anomaly [8]<sup>4</sup>, it is not difficult to show that the energy density of a BPS-saturated wall in SQCD satisfies a relation

$$\epsilon = \frac{N}{8\pi^2} \left| \langle \text{Tr } \lambda^2 \rangle_\infty - \langle \text{Tr } \lambda^2 \rangle_{-\infty} \right| \quad (1.4)$$

where the subscript  $\pm\infty$  marks the values of the gluino condensate at spatial infinities. The RHS of Eq.(1.4) presents an absolute lower bound for the energy of any field configuration interpolating between different vacua.

The relation (1.4) is valid *assuming* that the wall is BPS-saturated. However, whether such a BPS-saturated domain wall exists or not is a non-trivial dynamic question which can be answered only in a specific study of a particular theory in interest.

In Refs.[4, 10] this question was studied for the  $SU(2)$  gauge group in the framework of the effective low energy lagrangian due to Taylor, Veneziano, and Yankielowicz [11]. It is written in terms of the composite colorless chiral superfields

$$\Phi^3 = \frac{3}{32\pi^2} \text{Tr } \{W^2\}, \quad X^2 = S^f S_f \quad (1.5)$$

The effective *potential* is rigidly fixed from the requirement that the conformal and the chiral anomaly of the theory (1.1) under consideration are reproduced correctly. There is some freedom of choice for the kinetic term which we will discuss later in the paper. The effective TVY lagrangian presents a Wess-Zumino model with the superpotential

$$\mathcal{W} = \frac{2}{3} \Phi^3 \left[ \ln \frac{\Phi^3 X^2}{\Lambda_{SQCD}^5} - 1 \right] - \frac{m}{2} X^2 \quad (1.6)$$

The corresponding potential for the lowest components  $\phi, \chi$  of the superfields  $\Phi, X$

$$U(\phi, \chi) = \left| \frac{\partial \mathcal{W}}{\partial \phi} \right|^2 + \left| \frac{\partial \mathcal{W}}{\partial \chi} \right|^2 = 4 \left| \phi^2 \ln(\phi^3 \chi^2) \right|^2 + \left| \chi \left( m - \frac{4\phi^3}{3\chi^2} \right) \right|^2 \quad (1.7)$$

( from now on, with few exceptions, we will measure everything in the units of  $\Lambda_{SQCD} \equiv \Lambda$ ) has three non-trivial minima:

$$\phi = \chi = 0; \quad (1.8)$$

$$\begin{aligned} \phi &= \left( \frac{3m}{4} \right)^{1/6}, \quad \chi = \left( \frac{4}{3m} \right)^{1/4}; \\ \phi &= e^{-i\pi/3} \left( \frac{3m}{4} \right)^{1/6}, \quad \chi = i \left( \frac{4}{3m} \right)^{1/4} \end{aligned} \quad (1.9)$$

---

<sup>4</sup>See recent [9] for detailed pedagogical explanations.

There are also the minima with the inverse sign of  $\chi$  (and the appropriately chosen phase of  $\phi$ ), but they are physically the same as the minima (1.9): the vacuum expectation values of the gauge invariant operators  $\langle \text{Tr } \lambda^2 \rangle = (32\pi^2/3) \langle \phi^3 \rangle$  and  $\langle s^f s_f \rangle = \langle \chi^2 \rangle$  ( $s^f$  is the squark field) are the same. The vacua (1.9) involve a non-zero gluino condensate (1.2). The vacuum (1.8) is chirally symmetric.

To study the domain wall configurations, we should add to the potential (1.7) the kinetic term which we choose in the simplest possible form  $\mathcal{L}_{\text{kin}} = |\partial\phi|^2 + |\partial\chi|^2$  and solve the equations of motion with appropriate boundary conditions. In Ref.[4], it was done for the walls connecting a chirally asymmetric vacuum with the chirally symmetric one. It turned out that the solution exists for any value of  $m$  and that it is always BPS – saturated, i.e. the walls could be found solving not the equations of motion, but the more simple first order BPS equations (we again refer a reader to Ref.[9] for details)

$$\partial_z \phi = \pm \partial \bar{\mathcal{W}} / \partial \bar{\phi}, \quad \partial_z \chi = \pm \partial \bar{\mathcal{W}} / \partial \bar{\chi} \quad (1.10)$$

The surface energy density of these walls coincides with its lower bound (1.4). Explicitly, in physical units

$$\epsilon_0 = 4\sqrt{(m\Lambda_{SQCD}^5)/3} \quad (1.11)$$

However, there is also a different kind of walls which connect different chirally asymmetric vacua in (1.9)<sup>5</sup>. The BPS equations with the corresponding boundary conditions were solved numerically in [10]. It was shown that the solutions exist only in the limited range of masses  $m \leq m_* = 4.6705\dots$ . At larger masses, complex BPS domain walls *do* not exist. A kind of phase transition occurs.

In this paper, we perform a more detailed study of the complex walls. We show that on top of the *upper* BPS branch found in Ref.[4], also a *lower* BPS branch exists. Here the terms “upper” and “lower” refer not to energy (the energy of both branches is, of course, the same and is given by the BPS bound  $2\epsilon_0$ ), but to some other parameter: the value of  $|\phi|$  at the middle of the wall. When the mass is small, the trajectories can be found analytically. For the lower branch, the fields in the middle of the wall are very small in this case so that the wall presents a very loose bound state of two real walls. When the mass rises,  $|\phi|_{\text{middle}}$  also rises. At  $m = m_*$ , two branches fuse together.

We also studied numerically the wall solutions of the second order equations of motion. Some of the solutions are the BPS walls described above, but some are not. At  $m < m_*$ , there are two new *sphaleron* branches. They present saddle points of the energy functional. The upper (in the same sense as above) sphaleron branch presents

---

<sup>5</sup>We will call these walls *complex walls* in contrast to the *real walls* studied in Ref.[4]. For the walls separating the symmetric and an asymmetric vacua, the phase of the fields does not change. It can be set to zero which considerably simplifies the equations. For the walls separating different vacua in (1.9), the trajectories  $\phi(z)$  and  $\chi(z)$  are essentially complex, and the problem is technically more intricate.

a “mountain pass” between two different BPS valleys. The lower sphaleron branch presents a mountain pass between the lower BPS valley and the field configuration corresponding to two real BPS walls separated at infinite distance. At  $m = m_*$  when two BPS valleys fuse together, the upper sphaleron solution coincides with the BPS one: a mountain pass disappears and there is only one local minimum of the energy functional. This local minimum (and the corresponding solution for the equations of motion) exists also at somewhat larger masses, in the range  $m_* < m < m_{**}$ . It is not, however, a BPS - saturated minimum anymore, its energy somewhat exceeding the BPS bound. At  $m = m_* \approx 4.83$ , the upper branch fuses together with the lower sphaleron branch. At larger masses, *no complex domain wall solutions exist*.<sup>6</sup>

The plan of the paper is the following. Before proceeding with numerics, we discuss in the next section the limits  $m \rightarrow 0$  and  $m \rightarrow \infty$  where the problem can be studied analytically. In Sect.3, we describe in details the numerical solutions of the BPS equations in the intermediate mass range. In Sect.4, we solve the second order equations of motion and display the existence of two sphaleron branches. The last section is devoted to the discussion of physical relevance of our results and to some speculative remarks on the issues which are not yet clear.

## 2 Exploring the limits.

The situation is greatly simplified when the mass parameter  $m$  in the lagrangian (1.1) is large or small (compared to  $\Lambda$ ). Consider first the case of large masses. In this case, one can integrate the heavy matter fields out and write the effective lagrangian for the composite chiral superfield  $\Phi$ . Technically, one should use the Born–Oppenheimer procedure and to freeze down the matter field  $\chi$  so that the large second term in the potential (1.7) disappear. Proceeding in supersymmetric way, we get  $X^2 = 4\Phi^3/3m$ . Substituting it in the first term, we obtain the Veneziano–Yankielowicz effective lagrangian [12] which is the Wess–Zumino model for the single chiral superfield  $\Phi$  with the superpotential

$$\mathcal{W} = \frac{4}{3}\Phi^3 \left[ \ln \frac{\Phi^3}{\Lambda_{SYM}^3} - 1 \right] \quad (2.1)$$

where  $\Lambda_{SYM}^3 = \sqrt{3m\Lambda_{SQCD}^5}/4$ . The expression (2.1) and the corresponding expression for the potential

$$U(\phi) = |\partial\mathcal{W}/\partial\phi|^2 = 16|\phi^4| |\ln \phi^3|^2 \quad (2.2)$$

(here  $\phi$  is measured in the units of  $\Lambda_{SYM}$ ) is not yet well defined: the logarithm has many sheets, and one should specify first what particular sheet should be taken. An

---

<sup>6</sup>To avoid misunderstanding, we emphasize that two chirally asymmetric vacua can always be connected in two steps, via the symmetric one. That is there is always a “composite” solution presenting a combination of two real walls separated at infinite distance.

accurate analysis taking into account the fact that the topological charge

$$\nu = \frac{1}{16\pi^2} \int \text{Tr}\{G^2 \tilde{G}^2\} d^4x \quad (2.3)$$

in the original theory (1.1) is quantized to be integer reveals that the true potential is glued out of two pieces [2, 4]:

$$\begin{aligned} \ln \phi^3 &\equiv \ln |\phi^3| + i \arg(\phi^3), & \arg(\phi^3) &\in (-\pi/2, \pi/2) \\ \ln \phi^3 &\equiv \ln |\phi^3| + i[\arg(\phi^3) - \pi], & \arg(\phi^3) &\in (\pi/2, 3\pi/2) \end{aligned} \quad (2.4)$$

(remind that only the field  $\phi^3 \sim \text{Tr} \lambda^2$ , not  $\phi$  itself has a direct physical meaning). Quite an analogous situation holds in the Schwinger model: the true bosonized lagrangian (in the Schwinger model it is just *equivalent* to the original theory) is glued out of several branches when taking into account the effects due to quantization of topological charge [13]. The potential (2.2) has three degenerate minima. Two of them with  $\langle \text{Tr} \lambda^2 \rangle \propto \langle \phi^3 \rangle = \pm 1$  are chirally asymmetric and the third one with  $\langle \phi \rangle = 0$  is chirally symmetric.

The domain walls in this model were studied in [4]. It turned out that only the real domain walls interpolating between a chirally asymmetric and the chirally symmetric vacua exist in this case. Nontrivial complex domain wall solutions which do not go through zero are absent. Speaking of the real walls, they are BPS saturated and can be obtained solving the first order equations  $\partial\phi = \pm\partial\mathcal{W}/\partial\phi$ . The solution is “almost” analytical, it is expressed via integral logarithms.

Consider now the case of small masses. In this case, chirally asymmetric vacua are characterized by large values of the matter scalar field  $\chi$ . Again, the theory involves two different energy scales, and one can tentatively integrate out heavy fields and to write the Wilsonian effective lagrangian describing only light degrees of freedom. Proceeding in the Born–Oppenheimer spirit, we should freeze now the heavy field  $\phi$  in the potential (1.7) so that the large first term in the potential acquire its minimum (the zero) value. In contrast to the large mass situation, this can now be achieved in two ways: either by setting  $\phi = 0$  or by setting  $\phi^3 \chi^2 = 1$ . In the first case, we will obtain the effective lagrangian describing the dynamics of the chirally symmetric phase (it is just the lagrangian of free light chiral field  $X$  involving  $\chi$  and its superpartner).

The second choice results in the lagrangian describing the dynamics of the chirally asymmetric phases. It is the lagrangian of the Wess–Zumino model with a single chiral superfield  $X$  and a non-trivial superpotential

$$\mathcal{W} = -\frac{2}{3X^2} - \frac{m}{2}X^2. \quad (2.5)$$

This lagrangian is well known and was obtained earlier from instanton and/or from holomorphy considerations [1]. The corresponding potential  $U = |\partial\mathcal{W}/\partial\chi|^2$  has two different non-trivial minima at

$$\langle \chi^2 \rangle = \pm\chi_*^2 = \pm\sqrt{4/3m} \quad (2.6)$$

When  $m \ll 1$ , large expectation value (2.6) results in breaking down the gauge symmetry of the original theory by the Higgs mechanism: the theory is in the Higgs phase.

A domain wall interpolating between two vacua (2.6) is BPS-saturated. The solution can be found analytically [4]

$$\chi(z) = \chi_* \frac{1 + ie^{4m(z-z_0)}}{\sqrt{1 + e^{8m(z-z_0)}}} \quad (2.7)$$

where  $z_0$  is the position of the wall center. We see that  $|\chi(z)|$  stays constant and only the phase is changed.

In this approach, we are not able, however, to study the real domain walls interpolating between the chirally symmetric and a chirally asymmetric vacua. Such a wall corresponds to going through a high energy barrier separating two kind of vacua. It is a remarkable consequence of supersymmetry and of the related BPS condition (1.4) that the energy of such a wall is still not large.

It was shown in [4] that in the limit  $m \rightarrow 0$ , the real wall trajectory can also be found analytically. In a funny way, the transition from the chirally symmetric to a chirally asymmetric vacuum goes in two stages. On the first stage, only the field  $|\chi|$  is changed rising from zero at  $z = -\infty$  to its maximal value  $\chi_*$  at  $z = 0$ ,  $\chi(z) = \chi_* e^{mz}$ , while the field  $\phi$  stays frozen at zero. This first part of the wall has the width  $\sim 1/m$  and carries the half of the wall total energy. At  $z > 0$ , the trajectory abruptly turns.  $\chi(z)$  is not changed anymore, but  $\phi(z)$  changes until it levels off at its value in the asymmetric vacuum state  $\phi_* = \chi_*^{-2/3}$ . The equations for this second stretch have exactly the same form as the BPS equations in the pure supersymmetric Yang–Mills theory. The second part of the wall carries another half of the total energy, but is much thinner than the first part, its width being of order  $m^{-1/6}$ . It is on this second stage when the potential barrier between symmetric and asymmetric vacua is penetrated.

Thereby, the physical situation in the limits  $m \rightarrow 0$  and  $m \rightarrow \infty$  is somewhat different. In both cases, we have 3 different vacua. However, an analog of nontrivial complex walls (2.7) connecting different asymmetric vacua which are present at small masses, are absent when the mass is large. In the latter case, only real walls are present. It is therefore very interesting to understand what happens in between, at intermediate values of masses, and how the transition from one regime to another occurs. That was the main motivation for our study.

Generally, one should study the theory with the potential (1.7). The status of this effective theory is somewhat more uncertain than that of (2.5) — for general value of mass, the TVY effective lagrangian is not Wilsonian; light and heavy degrees of freedom are not nicely separated. But it possesses all the relevant symmetries of the original theory and satisfies the anomalous Ward identities for correlators at zero momenta. We think that the use of the TVY lagrangian is justified as far as the vacuum structure of the theory is concerned.

### 3 Solving BPS equations.

Let us choose the positive sign in Eq.(1.10) and try to solve it with the boundary conditions

$$\begin{aligned}\phi(-\infty) &= \left(\frac{3m}{4}\right)^{1/6}, \quad \phi(\infty) = e^{-i\pi/3} \left(\frac{3m}{4}\right)^{1/6}, \\ \chi(-\infty) &= \left(\frac{4}{3m}\right)^{1/4}, \quad \chi(\infty) = i \left(\frac{4}{3m}\right)^{1/4}\end{aligned}\tag{3.1}$$

(the negative sign in (1.10) would describe the wall going in the opposite direction in  $z$ ). The solution of the equations (1.10) with the boundary conditions (3.1) has the fixed energy density which due to (1.4) is twice as large as the energy density of the real wall (1.11). Thereby a complex BPS wall may be thought of as a marginaly stable bound state of two real walls.

Technically, it is convenient to introduce the polar variables  $\chi = \rho e^{i\alpha}$ ,  $\phi = R e^{i\beta}$ . Then the system (1.10) (with the positive sign chosen) can be written in the form

$$\begin{cases} \partial_z \rho = -m\rho \cos(2\alpha) + \frac{4R^3}{3\rho} \cos(3\beta) \\ \partial_z \alpha = m \sin(2\alpha) - \frac{4R^3}{3\rho^2} \sin(3\beta) \\ \partial_z R = 2R^2 [\cos(3\beta) \ln(R^3 \rho^2) - \sin(3\beta)(3\beta + 2\alpha)] \\ \partial_z \beta = -2R [\sin(3\beta) \ln(R^3 \rho^2) + \cos(3\beta)(3\beta + 2\alpha)] \end{cases}\tag{3.2}$$

The wall solution should be symmetric with respect to its center. Let us seek for the solution centered at  $z = 0$  so that

$$\rho(z) = \rho(-z), \quad R(z) = R(-z), \quad \alpha(z) = \pi/2 - \alpha(-z), \quad \beta(z) = -\pi/3 - \beta(-z)\tag{3.3}$$

Indeed, one can be easily convinced that the Ansatz (3.3) goes through the equations (3.2).<sup>7</sup>

The system (1.10) has one integral of motion [9]:

$$\text{Im } \mathcal{W}(\phi, \chi) = \text{const}\tag{3.4}$$

Indeed, we have

$$\partial_z \mathcal{W} = \frac{\partial \mathcal{W}}{\partial \phi} \partial_z \phi + \frac{\partial \mathcal{W}}{\partial \chi} \partial_z \chi = \left| \frac{\partial \mathcal{W}}{\partial \phi} \right|^2 + \left| \frac{\partial \mathcal{W}}{\partial \chi} \right|^2 = \partial_z \bar{\mathcal{W}}$$

It is convenient to solve the equations (3.2) numerically on the half-interval from  $z = 0$  to  $z = \infty$ . The symmetry (3.3) dictates  $\alpha(0) = \pi/4$ ,  $\beta(0) = -\pi/6$ . Then the condition (3.4) [in our case  $\text{Im } \mathcal{W}(\phi, \chi) = 0$  due to the boundary conditions (3.1)] implies

$$\frac{4R(0)^3}{3} \left\{ \ln[R(0)^3 \rho(0)^2] - 1 \right\} + m\rho(0)^2 = 0\tag{3.5}$$

---

<sup>7</sup>A logical possibility could be that symmetric equations have a couple of asymmetric solutions. We searched for such but did not find any, however.



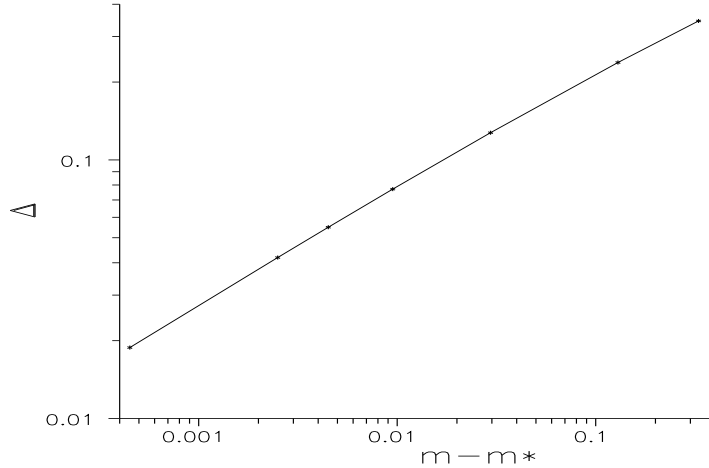


Figure 1: Mismatch parameter  $\Delta$  as a function of mass

Thus, only one parameter at  $z = 0$  [say,  $R(0)$ ] is left free. We should fit it so that the solution would approach the complex minimum in Eq.(1.9) at  $z \rightarrow \infty$ .

It turns out that the solution of this problem exists, but only in the limited range of  $m$ . If  $m > m_* = 4.67059\dots$ , the solution *misses* the minimum no matter what the value of  $R(0)$  is chosen. This is illustrated in Fig. 1 where the “mismatch parameter”

$$\Delta = \min_{R(0)} \min_z \sqrt{|\chi(z) - i(4/3m)^{1/4}|^2 + |\phi(z) - e^{-i\pi/3}(3m/4)^{1/6}|^2} \quad (3.6)$$

is plotted (in the double logarithmic scale) as a function of mass. The dependence  $\Delta(m)$  fits nicely the law

$$\Delta_{\text{BPS}}(m) = 0.56(m - m_*)^{0.44} \quad (3.7)$$

It smells like a critical behavior but, as  $\Delta$  is not a physical quantity, we would not elaborate this point further.

At  $m = 4.67059$  or at smaller values of mass, the solution exists, however. Moreover, it turns out that, at  $m < m_*$ , there are *two* different solutions: the upper branch with the larger value of  $R(0)$  and the lower branch with the lower value. In Fig. 2 we plotted the dependence of  $\eta = R(0)/R(\infty)$  on  $m$  for both branches. We see that, at  $m = m_*$ , two branches are joined together. This *is* the reason why no solution exists at larger masses.

Let us discuss now what happens with these two branches in the small mass limit. Consider first the upper branch. The profiles of the functions  $\rho(z)$  and  $R(z)$  for three values of mass:  $m = 0.01$ ,  $m = 2.0$ , and  $m = 4.67059$  for the upper branch

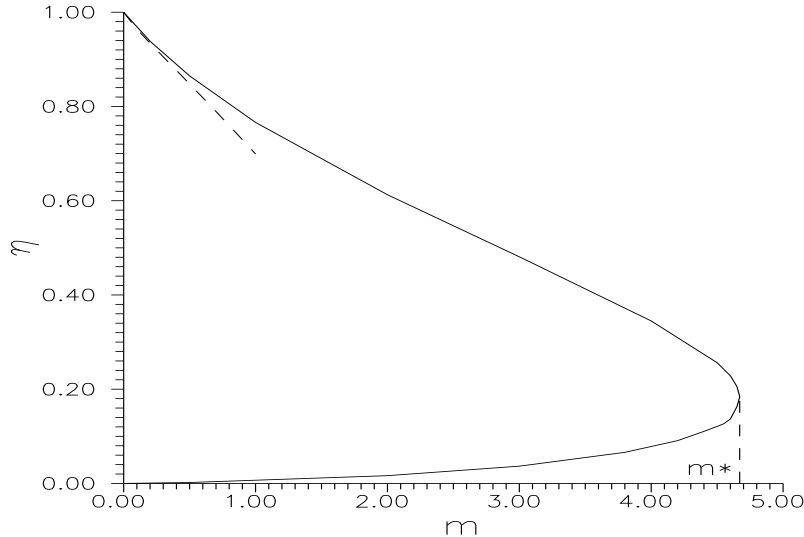


Figure 2: The ratio  $\eta = R(0)/R(\infty)$  as a function of mass. The dashed line describes the analytic result (3.8) valid for small masses.

in the whole interval  $-\infty < z < \infty$  are plotted in Figs. 3,4. We see that, for small masses,  $R(z)$  and  $\rho(z)$  are virtually constant. This is not surprising, of course. For small masses, the solution approaches, as it should, the analytic solution (2.7) (with  $\phi = \chi^{-2/3}$ ).

Linearizing at small nonzero masses the equations (3.2) with respect to small deviations of the solutions  $\Delta\rho(z), \Delta\alpha(z)$ , etc. from the analytic result (2.7) ( and  $\phi = \chi^{-2/3}$ ) valid in the limit  $m \rightarrow 0$ , it is possible to determine the dependence  $\eta(m)$  in the small mass region. The derivation in the general  $SU(N)$  case will be presented in [14]. Here we only quote the result for  $SU(2)$  :

$$\eta(m) = 1 - \frac{2}{9} \left( \frac{4m^5}{3} \right)^{1/6} - \frac{5}{81} \left( \frac{4m^5}{3} \right)^{1/3} + O(m^{5/2}) \quad (3.8)$$

The numerical results for  $\eta(m)$  are in the excellent agreement with this formula.

Consider now the lower branch.  $R_{\text{low}}(0)$  and, due to Eq.(3.5), also  $\rho_{\text{low}}(0)$  go to zero in the limit  $m \rightarrow 0$ . Thereby, the solution looks very much similar to a combination of two real walls separated at a large distance (The phases  $\alpha(z)$  and  $\beta(z)$  are changed, of course, so that the whole solution is complex, but the change occurs in the central region where the absolute values of the fields  $R$  and  $\rho$  are very small.). One can say that it is a very loosely bound state of two real walls. The profile  $\rho(z)$  for the lower BPS branch at  $m = .5$  found numerically is shown in Fig. 5. Indeed, the complex wall is split apart in two widely separated real walls.  $\rho(0) \approx 6.7 \cdot 10^{-4}$  in this case. We observe numerically that, for small masses,  $\rho(0)$  and  $R(0)$  go down  $\propto \exp\{-C/m^\alpha\}$  with  $\alpha \approx 1/4$ ,  $C_\rho \approx 6.1$ ,  $C_R \approx 5.3$ .

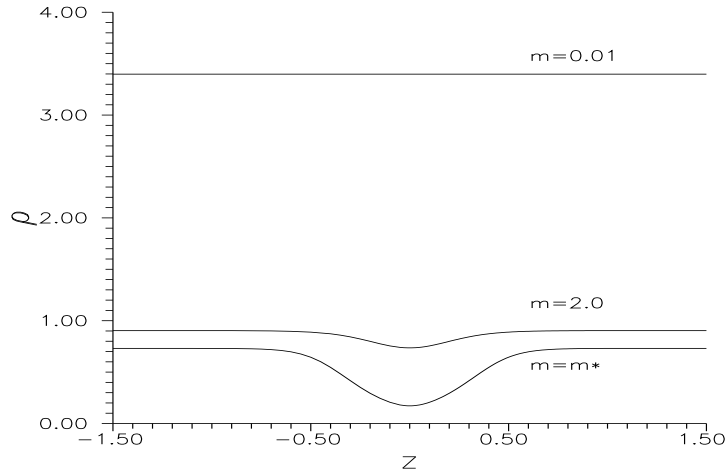


Figure 3: Upper BPS branch:  $\rho(z)$  for different masses.

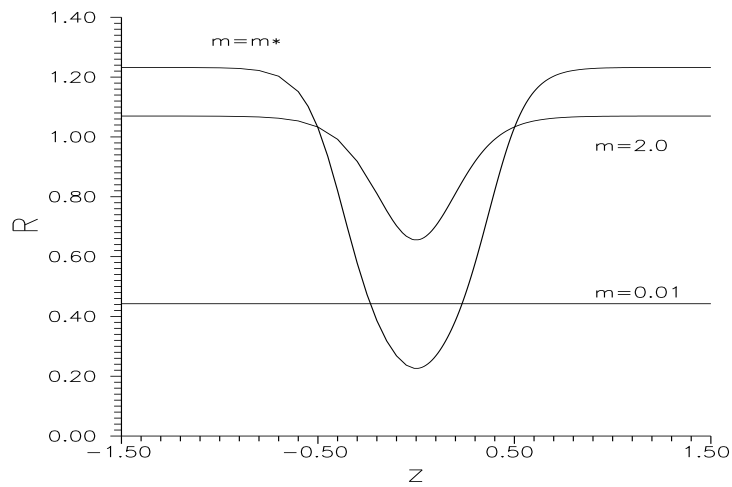


Figure 4: Upper BPS branch:  $R(z)$  for different masses.

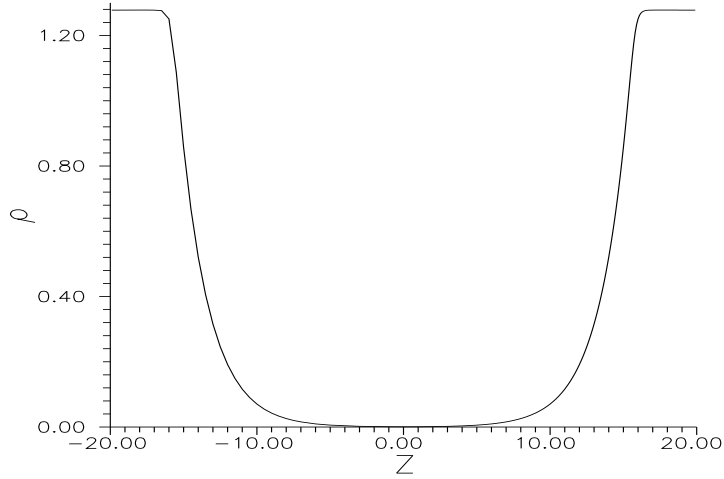


Figure 5: Profile  $\rho(z)$  of the lower BPS branch at  $m = 0.5$

The revealed phenomenon — the appearance of two solutions of the equation system (3.2) at  $m < m_*$  and the absence of solutions at  $m > m_*$  can be understood in the framework of the qualitative theory of differential equations (see Ref.[6] for a related discussion). The phase space of the system (3.2) is 4–dimensional. The space of all possible integral curves is 3–dimensional (there are 4 integration constants, but one of them corresponds to shifting the independent variable  $z$  along the trajectory).

The system involves the integral of motion (3.4) so that the whole 3–dimensional space of the trajectories presents a set of 2–dimensional slices with a given value of  $\text{Im } \mathcal{W}$ .

We are interested in a special trajectory belonging to the slice with  $\text{Im } \mathcal{W} = 0$  and passing through two chirally asymmetric minima (1.9). These minima present singular points of the equation system (3.2) where the right hand sides of the equations turn to zero. Thereby, the alias for our domain walls is *separatrices*.

Linearizing the equations at the vicinity of singular points and studying the matrix of the linear system thus obtained (the Jacobi matrix), one can be convinced that these points have saddle nature: the Jacobi matrix has two positive  $\lambda, \mu$  and two negative  $-\lambda, -\mu$  eigenvalues. The space of all possible trajectories which have their origin at one of the singular points (say, the point with real  $\phi, \chi$ ) is 1–dimensional — only the directions in the phase space along the eigenvectors of the Jacobi matrix with *positive* eigenvalues should be taken into account. There are two such eigenvectors which can be mixed with 1 real parameter. Likewise, the subspace of the trajectories which end up at the point  $\phi = e^{-i\pi/3}(3m/4)^{1/6}$ ,  $\chi = i(4/3m)^{1/4}$  is also 1–dimensional. They correspond to a mixture of two eigenvectors of the corresponding Jacobi matrix with *negative* eigenvalues. The wall solution belongs to

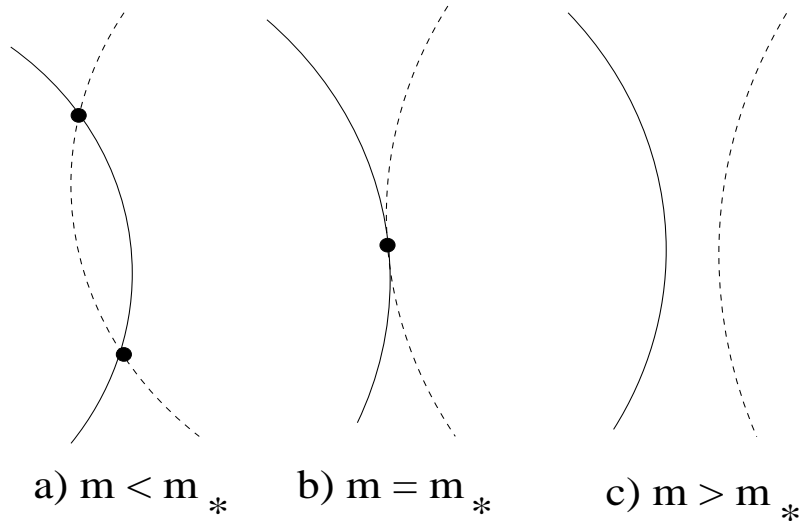


Figure 6: A space of trajectories with  $\text{Im } \mathcal{W} = 0$  for different masses. The solid lines describe the subspace of separatrices originating at one of the minima while the dashed lines describe the subspace of separatrices ending up at another minimum.

both subspaces.

Generally, two 1-dimensional lines embedded in the 2-dimensional space (the space of all trajectories with  $\text{Im } \mathcal{W} = 0$ ) can cross at a finite number of points. What is this number and whether the lines cross at all depends on dynamics. We have found the presence of two intersections at  $m < m_*$ , of one intersection at  $m = m_*$  and the absence of intersections at  $m > m_*$ . This picture illustrated schematically in Fig. 6 looks quite natural.<sup>8</sup>

---

<sup>8</sup>It is instructive to compare the situation with that in the model analyzed recently in Ref.[15] where a family of degenerate BPS wall solutions was observed. The model involved two chiral superfields with the superpotential

$$W = \frac{m^2}{\lambda} \Phi - \frac{\lambda}{3} \Phi^3 - \alpha \Phi X^2$$

BPS system involves here 4 singular points (4 vacua of the theory): two saddles, a stable and an unstable focuses. The BPS walls run from the instable focus to the stable one. Again, the families of the relevant separatrices are 1-dimensional. As in our case, the family of *all* trajectories is 3-dimensional. Here, however, the wall solutions lie in the one-dimensional subspace of the *real* trajectories satisfying the two conditions  $\text{Im } \Phi = 0$  and  $\text{Im } X = 0$  (all the vacua are real here). Hence, the space of the BPS wall solutions is  $1 + 1 - (3 - 2) = 1$ -dimensional.

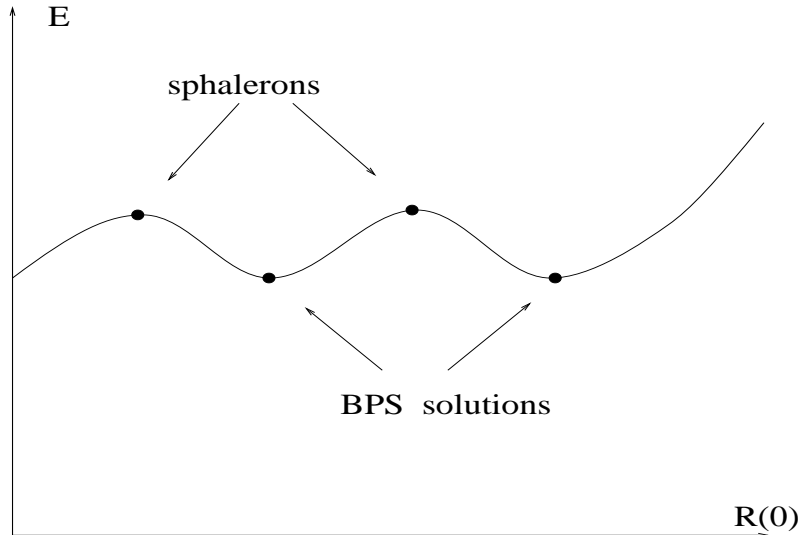


Figure 7: Stationary points of the energy functional,  $m < m_*$ .

## 4 Wallsome Sphalerons.

The BPS solutions realize the absolute minimum of the energy functional for all wall configurations. The other configurations have larger energy. In the region  $m < m_*$ , we have found two different BPS solutions which should be separated by an energy barrier. Besides two nontrivial complex wall solutions, there is always a configuration describing two real walls separated at infinite distance. The energy of such a configuration is twice the energy of the real wall which coincides in our  $[SU(2)]$  case with the energy of the complex wall. There should be also an energy barrier separating this configuration from the lower BPS solution. This situation is illustrated in Fig. 7 where the energy functional minimized over all symmetric wall configurations with a fixed value of  $R(0)$  (the value of  $|\phi|$  in the middle) is drawn schematically as a function of  $R(0)$ . We see that besides the minima (the BPS solutions), this plot has local maxima. In fact, they are the saddle points of the energy functional with only one unstable mode corresponding to changing  $R(0)$ . Such saddle point configurations (the sphalerons) present non-trivial solutions of the equations of motion. They are not BPS solutions, of course.

Thus, to study sphalerons, we should solve the full-scale second order equations of motion for the effective lagrangian with the potential (1.7)<sup>9</sup> and the standard kinetic term. Introducing again the polar variables  $\chi = \rho e^{i\alpha}$ ,  $\phi = R e^{i\beta}$ , the

<sup>9</sup>As usual, the sign of the potential should be reversed: we are looking for the minimum of the energy functional, not the action functional.

equations can be written in the form

$$\begin{aligned}
R'' - R\beta'^2 &= 8R^3[L(L + 3/2) + \beta_+^2] + \frac{16R^5}{3\rho^2} - 4mR^2 \cos(\beta_-) \\
R\beta'' + 2R'\beta' &= 12R^3\beta_+ + 4mR^2 \sin(\beta_-) \\
\rho'' - \rho\alpha'^2 &= \frac{8R^4}{\rho}L + m^2\rho - \frac{16R^6}{9\rho^3} \\
\rho\alpha'' + 2\rho'\alpha' &= \frac{8R^4}{\rho}\beta_+ - \frac{8mR^3}{3\rho} \sin(\beta_-) \tag{4.1}
\end{aligned}$$

where  $L = \ln(R^3\rho^2)$ ,  $\beta_{\pm} = 3\beta \pm 2\alpha$ . The system (4.1) involves one integral of motion

$$\begin{aligned}
T - U &= R'^2 + R^2\beta'^2 + \rho'^2 + \rho^2\alpha'^2 - \\
\left[ 4R^4(L^2 + \beta_+^2) + m^2\rho^2 + \frac{16R^6}{9\rho^2} - \frac{8mR^3}{3} \cos(\beta_-) \right] &= \text{const} \tag{4.2}
\end{aligned}$$

Solving the system (4.1) is a more complicated technical problem than that for the BPS system (3.2). The Cauchy problem involves here 8 initial conditions. As earlier, we can restrict our search with the symmetric configurations [see Eq.(3.3)]. Then 4 initial conditions are fixed:

$$R'(0) = 0, \quad \rho'(0) = 0, \quad \alpha(0) = \pi/4, \quad \beta(0) = -\pi/6$$

Four other initial values satisfy the relation (4.2) with  $const = 0$ . Thus, we are left with 3 free parameters, say,  $\rho(0)$ ,  $R(0)$ , and  $\beta'(0)$ , which should be fitted so that the solution approach the complex vacuum in Eq.(1.9) at  $z \rightarrow \infty$ . Technically, we used the mismatch parameter in Eq.(3.6) as a criterium, the initial data were fitted to minimize it.

The results are presented in Fig. 8. We obtain first of all our old BPS solutions (solid lines in Fig.8). We find also two new solution branches drawn with the dashed lines in Fig. 8. We see that, similarly to the BPS branches, two new dashed branches fuse together at some  $m = m_{**} \approx 4.83$ .<sup>10</sup> No solution for the system (4.1) exists at  $m > m_{**}$ . For large masses, the minimal mismatch parameter  $\Delta$  defined in Eq.(3.6) is not zero, and the larger is  $m - m_{**}$ , the larger  $\Delta$  is. Numerically, we find in this case

$$\Delta_{\text{eq.mot.}}(m) = 0.052(m - m_{**})^{0.82} \tag{4.3}$$

in the full analogy with Eq.(3.7).

<sup>10</sup>To be on the safe side, we would claim  $m_{**} = 4.835 \pm .020$ . The accuracy here is much lower than that for  $m_*$  precisely because looking for the minimum of  $\Delta$  in the space of 3 parameters is much more complicated numerical problem than fitting just 1 parameter which we did while searching for BPS solutions. That is also the reason why the dashed branches are not drawn in the region of small masses. Our accuracy is not sufficient there.

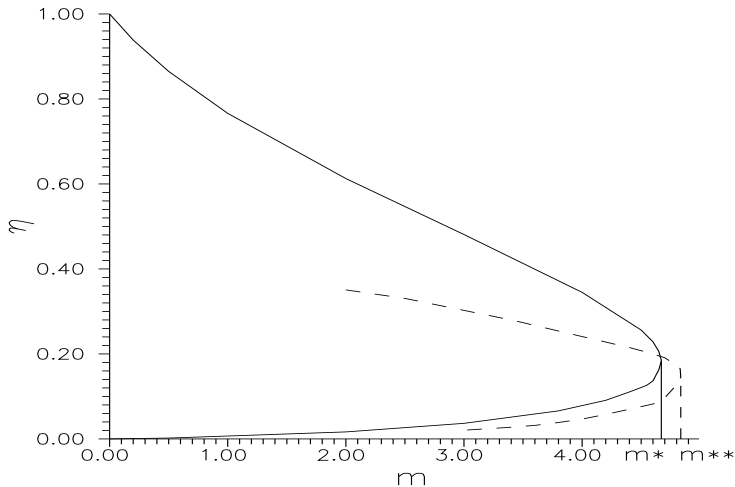


Figure 8: The solutions of equations of motion at different masses. Solid lines correspond to the BPS solutions and dashed lines — to the sphalerons or non-BPS local minima.

The physical interpretation of these new solutions is rather transparent. For  $m < m_*$ , they present the sphalerons as shown in Fig. 7. At  $m = m_*$ , two BPS minima fuse together and the energy barrier separating them disappears. The upper sphaleron branch meets with the BPS branches at this point. When  $m$  is slightly above  $m_*$ , the former BPS minimum is still a local minimum of the energy functional, but its energy is now slightly above the BPS bound (see Fig. 9a). The corresponding solution is described by the analytic continuation of the upper sphaleron branch. The lower dashed branch in the region  $m_* < m < m_{**}$  is still a sphaleron. At the second critical point  $m = m_{**}$ , the picture is changed again (see Fig. 9b). The local maximum and the local minimum fuse together and the only one remaining stationary point does not correspond to an extremum of the energy functional anymore. At larger masses, no non-trivial stationary points are left.

Like in the simpler BPS case, the presence of the discrete number of the wall solutions for the system (4.1) depending on the value of the parameter  $m$  can be naturally interpreted in the language of the qualitative theory of differential equations. The phase space is now 8-dimensional and the space of all *trajectories* is 7-dimensional. There is one integral of motion (4.2) and our wall solutions belong to the 6-dimensional subspace of the trajectories with  $T - U = 0$ . Again, the minima (1.9) with zero derivatives  $\dot{\phi} = \dot{\chi} = 0$  present the critical points of the equation system (4.1). The corresponding  $8 \times 8$  Jacobi matrices involve 4 positive and 4 negative eigenvalues [the eigenvalues are actually the same as for the BPS system (3.2), but each eigenvalue is now double degenerate]. Thereby, the family of separatrices which go down from one of the critical points is 3-dimensional. The



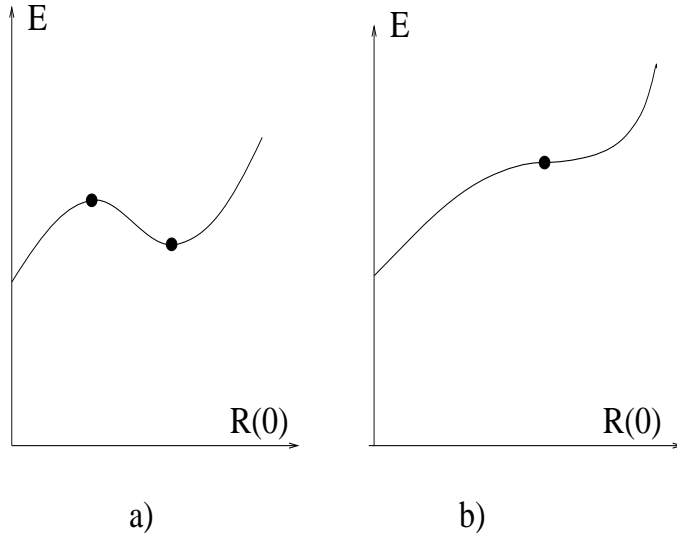


Figure 9: Stationary points of the energy functional: a)  $m_* < m < m_{**}$ , b)  $m = m_{**}$ .

same is true for the family of separatrices which end up at the other minimum. Generally, two 3-dimensional manifolds embedded in the 6-dimensional space of all trajectories with  $T - U = 0$  may cross at a finite number of points. We have seen that the crossing occurs at 4,2,1, or 0 points depending on the value of mass. This looks reasonable though in this case we are not clever enough to visualize it.

We hasten to comment that the height of the energy barrier as shown in Figs. 7, 9 is very much exaggerated. In fact, we could not even accurately determine the difference of the energy of the lower sphaleron branch and of all the dashed branches in the intermediate mass region  $m_* < m < m_{**}$  from the BPS bound  $\epsilon_{BPS}$ . We can only say that the relative difference  $\kappa = (\epsilon - \epsilon_{BPS})/\epsilon_{BPS}$  is well below  $10^{-4}$  in this case. The appearance out of the blue of such a small number which is not present neither in supersymmetric QCD lagrangian nor in the effective TVY theory is rather surprising. Right now we do not see a profound theoretical reason for this “experimental fact”, but the numerical evidence is unequivocal. The fact that the barrier is very low conforms well with the fact that the second phase transition occurs pretty soon after the first one: the values  $m_* \approx 4.67$  and  $m_{**} \approx 4.83$  are very close.

The difference of the energy of the upper sphaleron from the BPS bound can be numerically evaluated in a certain mass region. The results are plotted in Fig. 10. Naturally, the height of the barrier goes to zero when  $m$  approaches  $m_*$ . But, as seen from Fig. 10, even at small masses, the barrier height is still rather small. In the range of  $m_* - m$  where we could calculate  $\kappa$  reliably, it follows nicely the fit  $\kappa \approx 3.90 \cdot 10^{-5} \exp\{1.74(m_* - m)\}$  (the dashed line in Fig. 10)

Finally, we present for illustration the profiles  $R(z)$  for all four branches at  $m = 3$

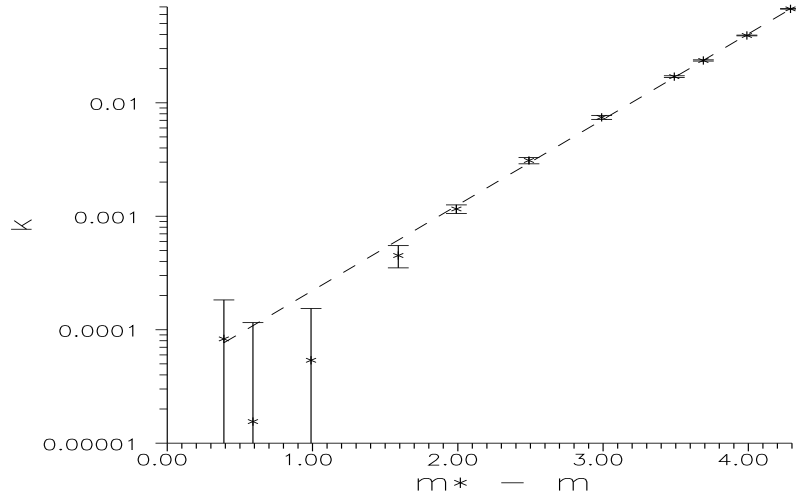


Figure 10: Energy of the upper sphaleron as a function of mass.

(see Fig. 11).

## 5 Discussion.

We have found that the properties of the system are drastically changed at  $m = 4.67059\dots\Lambda$  and further at  $m \approx 4.83\Lambda$ . It makes sense to express the result in invariant terms and to trade  $\Lambda$  for an invariant physical quantity such as the gluino condensate  $\Sigma = | \langle \text{Tr } \lambda^2 \rangle |$  in a chirally asymmetric vacuum. From Eqs.(1.9), (1.5), we obtain

$$\Sigma = \frac{16\pi^2}{\sqrt{3}} m^{1/2} \Lambda^{5/2} \quad (5.1)$$

Thus, the phase transitions occur at

$$m_* \approx m_{**} \approx 0.8\Sigma^{1/3} \quad (5.2)$$

Needless to say, they are not phase transitions of a habitual thermodynamic variety. In particular, the vacuum energy is zero both below and above the phase transition point — supersymmetry is never broken here. Hence  $E_{vac}(m) \equiv 0$  is not singular at  $m = m_*, m_{**}$ . Some similarities may be observed with the 2-dimensional Sine-Gordon model where the number of the states in the spectrum depends on the coupling constant  $\beta$  so that the states appear or disappear at some critical values of  $\beta$  [16]. May be a more close analogy can be drawn with the  $N = 2$  supersymmetric Yang-Mills theory. The spectrum of that system depends on the Higgs expectation

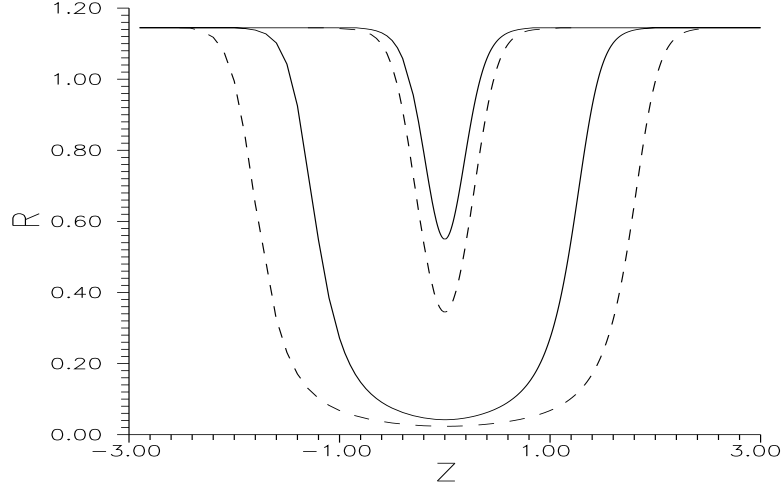


Figure 11: Profiles  $R(z)$  for BPS walls (solid lines) and wallsome sphalerons (dashed lines) for  $m = 3$ .

value  $u = \langle \text{Tr } \varphi^2 \rangle$ . A study of the exact solution of the model due to Seiberg and Witten [17] displays the existence of a “marginal stability curve” in the complex  $u$ -plane [18]. When crossing this curve, the spectrum pattern is qualitatively changed.

The particular numerical value (5.2) was obtained by studying the effective TVY lagrangian with the superpotential (1.6) and the standard kinetic term  $|\partial\phi|^2 + |\partial\chi|^2$  which follows from the term  $\frac{1}{4} \int d^4\theta (\bar{\Phi}\Phi + \bar{X}X)$  in the superlagrangian. However, in contrast to the superpotential, the form of the kinetic term in the effective lagrangian cannot be fixed from the symmetry considerations alone. As an obvious generalization, one can write

$$\mathcal{L}_{\text{kin}} = \frac{\alpha}{4} \int d^4\theta \bar{\Phi}\Phi + \frac{\beta}{4} \int d^4\theta \bar{X}X \quad (5.3)$$

Adding the term  $\frac{1}{2} \int \mathcal{W}(\Phi, X) d^2\theta + \text{H.c.}$  and excluding the auxiliary fields, the bosonic part of the lagrangian acquires the form

$$\mathcal{L} = \alpha |\partial\phi|^2 + \beta |\partial\chi|^2 - \frac{1}{\alpha} \left| \frac{\partial\mathcal{W}}{\partial\phi} \right|^2 - \frac{1}{\beta} \left| \frac{\partial\mathcal{W}}{\partial\chi} \right|^2 \quad (5.4)$$

The BPS equations are modified to

$$\alpha \frac{\partial\phi}{\partial z} = \pm \frac{\partial\bar{\mathcal{W}}}{\partial\bar{\phi}}, \quad \beta \frac{\partial\chi}{\partial z} = \pm \frac{\partial\bar{\mathcal{W}}}{\partial\bar{\chi}}, \quad (5.5)$$

Suppose first that  $\alpha = \beta$ . Then the equations (5.5) can be reduced in the standard form (1.10) by rescaling the independent variable  $z = \alpha z'$ . The walls become thicker

(or thinner) but, in all other respects, the form and the properties of the solutions are the same. If  $\alpha \neq \beta$ , the situation is not so trivial. The corresponding effective lagrangian seems to describe a different dynamics than that with  $\alpha = \beta = 1$ . Nevertheless, we will shortly see that the lagrangian (5.4) can still be reduced to the lagrangian with the standard kinetic term by rescaling *both* the independent variable  $z$  *and* the mass parameter  $m$ .

Suppose, we have already set  $\alpha = 1$  by rescaling  $z$  in a proper way. It is not difficult to see that the BPS system (5.5) is reduced to the standard system (1.10) with the superpotential

$$\mathcal{W} = \frac{2}{3}\Phi^3 \left[ \ln \frac{\Phi^3 X'^2}{\beta \Lambda^5} - 1 \right] - \frac{m}{2\beta} X'^2 \quad (5.6)$$

where  $X' = \beta^{1/2} X$ . The expression (5.6) has the same functional form as Eq.(1.6), only the scales for  $\Lambda$  and  $m$  have changed. Again, the BPS solutions disappear when  $m > m_*(\beta) = 4.67059 \dots \beta^{6/5}$ . In physical units,  $m_*(\beta) \approx 0.8\beta\Sigma^{1/3}$ . The second critical point scales in the same way.

Thus, we cannot claim that the phase transition in the theory of interest (1.1) would occurs exactly at the mass (5.2). Our guess, however, is that the true values of  $m_*$  and  $m_{**}$  in the supersymmetric QCD are close to the estimate (5.2).<sup>11</sup>

To summarize, our main physical conclusion is the absence of complex domain walls connecting different chirally asymmetric vacua in the supersymmetric QCD at large enough masses. In particular, they are absent in the limit  $m \rightarrow \infty$ , for the pure supersymmetric Yang–Mills theory.

In recent [19], the complex domain walls in the pure  $N = 1$  SYM theory were discussed in the context of D–brane dynamics. It was shown, in particular, that these walls, in spite of the fact that, on the fundamental level, they are composed of the fundamental gluon and gluino fields in the adjoint representation of the gauge group, behave like objects in the fundamental representation in color. In particular, a QCD string originating at a heavy fundamental source may end up at the domain wall (cf. the analogous situation in the massless adjoint  $QCD_2$  where fundamental colored sources are screened in spite of the fact that the lagrangian of the theory does not involve the fields which are fundamental in color [20]). But that was in the *assumption* that such walls are there which, as we have seen, is not true.

The walls interpolating between a chirally asymmetric and the chirally symmetric vacua are present at any value of mass and also in the limit  $m \rightarrow \infty$ . For the time being, it is difficult for us to say something about their color properties: their very

---

<sup>11</sup>Of course, the modification (5.3) is not the only possible one. One could invent more complicated kinetic terms involving higher (covariant) derivatives and some fractional powers of  $\Phi$  and  $X$ . We did not study these exotic modifications and cannot exclude a logical possibility that, after adding the terms with high derivatives, physics would dramatically change: e.g. the complex BPS walls would exist at any value of mass or would not exist at all. We do not believe, however, that this possibility is realized.

existence has been detected only in the framework of the effective TVY lagrangian involving only colorless composite fields.

Finally, in the light of our new results, let us discuss the problem of torons. Torons are Euclidean gauge field configurations with fractional topological charge (2.3),  $\nu$  being the integer multiple of  $1/N$ , which may in principle contribute in the Euclidean path integral in the theory involving only adjoint color fields regularized in the infrared by placing it in a finite 4-dimensional toroidal box [21]. Whether such toron contributions are relevant or not in the supersymmetric gluodynamics is an old and controversial question (see e.g. [22]). It was discussed in details recently in [4], and we will not present here anew all the arguments *pro* and *contra*.

We would like only to reiterate here that the presence of torons would substantially modify the physical picture for the vacuum structure of the supersymmetric gluodynamics (vis.  $N + 1$  degenerate vacua and  $N$  different real domain walls interpolating between them) advocated in [4] and in the present paper. In the first place, the presence of torons would modify the gluing prescription for the effective potential (2.2). The gluing would occur at  $\arg(\phi^3) = \pi$  rather than at  $\arg(\phi^3) = \pi/2$  and  $\arg(\phi^3) = 3\pi/2$  as is the case when only the instanton-like gauge field configurations with integer topological charge are taken into account. Then the potential (2.2) would have only one non-trivial minimum at  $\arg(\phi^3) = 0$ , not two such minima as before. The theory would involve only two vacua, the chirally asymmetric and the chirally symmetric one, and only one interpolating domain wall.

We have seen, however, that, at least if the supersymmetric gluodynamics is understood as the supersymmetric *QCD* in the limit  $m \rightarrow \infty$ , this *is* not true. When the matter chiral multiplets are added, torons just do not exist however large the mass is (the Dirac equation for fundamental color fields does not make sense on a toron background), and the picture with 3 [ $N + 1$  for the  $SU(N)$  case] vacuum states *is* correct.

A nontrivial feature of the theory under consideration is that the *real* domain walls do not decouple in the limit  $m \rightarrow \infty$ . That is in contrast to the simple two-dimensional model discussed in Ref.[4] where the energy of a two-dimensional *analogue* of the 4-dimensional supersymmetric domain walls becomes infinite in the limit  $m \rightarrow \infty$  so that, in this limit, the vacua decouple completely from each other, and the physical picture corresponds not to the spontaneous breaking of a discrete symmetry, but to the appearance of a new *superselection rule* in the theory which just corresponds to the *analogue* of toron contributions in the path integral being switched on.

Note further that, for the supersymmetric *QCD* with large mass, the problem of how the different branches of logarithm in the potential are glued together is completely irrelevant as far as the wall solutions are concerned. For the real walls, we have always  $\arg(\phi^3 \chi^2) = 0$  irrespectively of whether  $\arg(\phi^3) = 0$  (for the wall connecting the vacuum with the positive value of  $\langle \text{Tr } \lambda^2 \rangle$  with the chirally symmetric one) or  $\arg(\phi^3) = \pi$  ( for the wall connecting the vacua with  $\langle \text{Tr } \lambda^2 \rangle < 0$  and  $\langle \text{Tr } \lambda^2 \rangle = 0$ ). The phase of the heavy field  $\chi$  always compensates the

phase of  $\phi$ . In a sense, heavy fields do not decouple *completely* in this case.

The question of whether it still makes sense to formulate the pure supersymmetric gluodynamics *not* as the large mass limit of supersymmetric  $QCD$  but in some other way which takes into consideration the toron contributions so that the theory would involve only *one* domain wall connecting *two* different vacua is still open. To clarify it, one should first try to understand better the dynamics of the chirally symmetric phase.

In fact, the existence of the chirally symmetric vacuum is probably the most interesting and unexpected result of the effective lagrangian approach. What is especially surprising is that it has the same (zero) energy as the chirally asymmetric vacua. Such degeneracy is not required by any symmetry considerations. Note that the degeneracy is there only for the theory defined at infinite volume. At small volumes when the effective gauge coupling is small, the theory can be analyzed directly in terms of the fundamental gluon and gluino fields, there are only  $N$  vacuum states with nonzero value of the condensate, and no trace of the chirally symmetric phase is seen [23]. By analyticity, that should be true also for large (but finite) volumes. Indeed, playing around with the finite volume formulas of Ref.[2] displays that the degeneracy is lifted also for large volumes, the energy gap going to zero exponentially fast in the limit  $L \rightarrow \infty$ .

There is a striking analogy with a two-dimensional model [ $QCD_2$  with the fermions in the adjoint color representation for higher unitary groups  $SU(N \geq 3)$ ] studied in Ref.[13]. In this model, the bosonized lagrangian displays the existence of several vacuum states separated presumably by the domain walls (the latter are just solitons in two dimensions). Like in the supersymmetric  $QCD_4$ , different vacua are distinguished by the different values of the fermion condensate  $\langle \text{Tr} \{ \lambda_R \lambda_L \} \rangle$ . For higher even  $N$ , the existence of several vacua does not follow from symmetry considerations (for odd  $N$ , it *does*). That was formulated as a paradox in Ref.[13] but, bearing in mind fresh insights from supersymmetric  $QCD_4$ , it looks now less surprising.

**Acknowledgments:** We are indebted to M. Shifman for useful comments and to N. Koniukhova for the interest and the advices concerning the numerical aspect of the problem. A.S. acknowledges warm hospitality extended to him at Saclay where this work was finished. This work was supported in part by the RFBR-INTAS grants 93-0283, 94-2851, and 95-0681, by the RFFI grants 96-02-17230, 97-02-17491, and 97-02-16131, by the RFBR-DRF grant 96-02-00088, by the U.S. Civilian Research and Development Foundation under award # RP2-132, and by the Schweizerischer National Fonds grant # 7SUPJ048716.

## References

- [1] V. Novikov, M. Shifman, A. Vainshtein, and V. Zakharov, *Nucl. Phys.* **B229** (1983) 407; *Phys. Lett.* **B166** (1986) 334; I. Affleck, M. Dine and N. Seiberg, *Nucl. Phys.* **B241** (1984) 493; **B256** (1985) 557. G. Rossi and G. Veneziano, *Phys. Lett.* **138B** (1984) 195; D. Amati, K. Konishi, Y. Meurice, G. Rossi and G. Veneziano, *Phys. Rep.* **162** (1988) 557; M. Shifman, *Int. J. Mod. Phys.* **A11** (1996) 5761.
- [2] A. Kovner and M. Shifman, hep-th/9702174 [Phys. Rev. D, to appear].
- [3] G. Dvali and M. Shifman, *Phys. Lett.* **B396** (1997) 64; hep-th/9611213 [Nucl. Phys. B, to appear].
- [4] A. Kovner, M. Shifman, and A. Smilga, hep-th/9706089 [Phys. Rev. D, to appear].
- [5] E. Witten and D. Olive, *Phys. Lett.* **B78**(1978) 97.
- [6] S. Cecotti and C. Vafa, *Commun. Math. Phys.* **158** (1993) 569.
- [7] E. Abraham and P. Townsend, *Nucl. Phys.* **B351** (1991) 313; M. Cvetič, F. Quevedo, and S.-J. Rey, *Phys. Rev. Lett.* **67** (1991) 1836.
- [8] K. Konishi, *Phys. Lett.* **B135** (1984) 439; K. Konishi and K. Shizuya, *Nuov. Cim.* **A90** (1985) 111.
- [9] B. Chibisov and M. Shifman, hep-th/9706141
- [10] A. Smilga and A. Veselov, hep-th/9706217 [ Phys. Rev. Lett., to appear].
- [11] T. Taylor, G. Veneziano and S. Yankielowicz, *Nucl. Phys.* **B218** (1983) 493.
- [12] G. Veneziano and S. Yankielowicz, *Phys. Lett.* **113B** (1982) 231.
- [13] A. Smilga, *Phys. Rev.* **D54** (1996) 7757.
- [14] A. Smilga, in preparation.
- [15] M. Shifman, hep-th/9708060; M. Shifman and M. Voloshin, hep-th/9709137.
- [16] R. Dashen, B. Hasslacher, and A. Neveu, *Phys. Rev.* **D11** (1975) 3424.
- [17] N. Seiberg and E. Witten, *Nucl. Phys.* **B426** (1994) 19; (E) **B430** (1994) 485.
- [18] F. Ferrari and A. Bilal, *Nucl. Phys.* **B169** (1996) 387.
- [19] E. Witten, hep-th/9706109.
- [20] D. Gross, I. Klebanov, A. Matsitsyn, and A. Smilga, *Nucl. Phys.* **B461** (1996) 109.

- [21] G. 't Hooft, *Comm. Math. Phys.* **81** (1981) 267.
- [22] E. Cohen and C. Gomez, *Phys. Rev* **52** (1984) 237; A.R. Zhitnitsky, *Nucl. Phys.* **B340** (1990) 56; H. Leutwyler and A.V. Smilga, *Phys. Rev.* **D46** (1992) 5607.
- [23] E. Witten, *Nucl. Phys.* **B202** (1982) 253.